

Towards Dynamic Resource Allocation and Client Scheduling in Hierarchical Federated Learning: A Two-Phase Deep Reinforcement Learning Approach

Xiaojing Chen, Zhenyuan Li, Wei Ni, *Fellow, IEEE*, Xin Wang, *Fellow, IEEE*, Shunqing Zhang, *Senior Member, IEEE*, Yanzan Sun, Shugong Xu, *Fellow, IEEE*, and Qingqi Pei, *Senior Member, IEEE*

Abstract—Federated learning (FL) is a viable technique to train a shared machine learning model without sharing data. Hierarchical FL (HFL) system has yet to be studied regarding its multiple levels of energy, computation, communication, and client scheduling, especially when it comes to clients relying on energy harvesting to power their operations. This paper presents a new two-phase deep deterministic policy gradient (DDPG) framework, referred to as “TP-DDPG”, to balance online the learning delay and model accuracy of an FL process in an energy harvesting-powered HFL system. The key idea is that we divide optimization decisions into two groups, and employ DDPG to learn one group in the first phase, while interpreting the other group as part of the environment to provide rewards for training the DDPG in the second phase. Specifically, the DDPG learns the selection of participating clients, and their CPU configurations and the transmission powers. A new straggler-aware client association and bandwidth allocation (SCABA) algorithm efficiently optimizes the other decisions and evaluates the reward for the DDPG. Experiments demonstrate that with substantially reduced number of learnable parameters, the TP-DDPG can quickly converge to effective policies that can shorten the training time of HFL by 39.4% compared to its benchmarks, when the required test accuracy of HFL is 0.9.

Index Terms—Hierarchical federated learning, resource allocation, client scheduling, deep deterministic policy gradient

I. INTRODUCTION

With the advent of the Internet-of-Things (IoT), pervasively deployed devices are revolutionizing the way we live and work, by producing vast amounts of data [1], [2]. Virtual reality, autonomous driving, and intelligent inference can be

enabled by applying deep learning to the rich data. As a collaborative decentralized machine learning paradigm, federated learning (FL) is becoming increasingly popular, where IoT devices, namely, clients, download global models from parameter servers, update their local models, and upload the local models for iterative global model updates to the parameter server [3]. Allowing the model to be updated locally, FL can protect sensitive local data [4] and substantially reduce the burden on network backbones since the models are typically much more lightweight than the data samples [5].

The key challenge of FL systems arises from restrictive resources, including finite (and limited) computing power and communication bandwidth, especially in the face of the straggler effect. The straggler effect occurs when each training round only progresses as fast as the slowest client in a synchronous FL process, since the central server has to wait for all clients to complete local training before a global aggregation can take place [5]. The slowest client is known as the straggler, which increases the training latency of FL. First, due to the limited bandwidth and heterogeneous clients, it is necessary to select appropriate clients to participate in FL and guarantee learning accuracy, while allocating the computation and communication resources efficiently to minimize the learning delay. Densely distributed clients can usually communicate with multiple edge servers, making client association decisions difficult. Moreover, the clients of FL, e.g., sensor nodes in remote areas, are usually powered by finite batteries. Effective energy management is critical to making full use of constrained batteries. As a result, joint optimization of energy, computation and communication resource allocation, and client scheduling is non-trivial to create effective FL.

Many existing FL studies [6]–[17] assumed a cloud server or an edge server as the parameter server, namely cloud- or edge-based FL. However, cloud-based FL can cause a large amount of delay and a high drop-out rate due to communication problems with the cloud server [6]. On the contrary, although edge-based FL can meet benefit from low latency and high reliability, its training performance inevitably declines due to relatively few clients that the edge server can access. A new client-edge-cloud hierarchical FL (HFL) system was recently proposed in [18], where edge servers serve as intermediaries between the cloud server and clients. Such a hierarchical architecture takes advantage of the cloud- and edge-based FL. On the one hand, the clients can send local models to the nearby edge servers rather than the cloud server for edge

Work in the paper was supported by the National Key R&D Program of China grants 2022YFB2902002 and 2022YFB2902303, the Innovation Program of Shanghai Municipal Science and Technology Commission grant 21ZR1422400, the Program of Hebei Key Laboratory of Advanced Laser Technology and Equipment grant HBKL-ALTE202401, the National High Quality Program grant TC220H07D, and Shanghai Rising-Star Program. (*Corresponding authors: Shunqing Zhang; Yanzan Sun.*)

X. Chen, Z. Li, S. Zhang, Y. Sun and S. Xu are with the Key Laboratory of Specialty Fiber Optics and Optical Access Networks, Shanghai University, Shanghai 200444, China. Emails: {jodiechen, fivears, shunqing, yanzansun, shugong}@shu.edu.cn.

W. Ni is with the Commonwealth Scientific and Industrial Research Organization (CSIRO), Sydney, NSW 2122, Australia. Email: wei.ni@data61.csiro.au.

X. Wang is with the Key Laboratory of EMW Information (MoE), the Department of Communication Science and Engineering, Fudan University, Shanghai 200433, China. Email: xwang11@fudan.edu.cn.

Q. Pei is with the State Key Laboratory of Integrated Services Networks, School of Telecommunications Engineering, Xidian University, Xi’an 710071, China. Email: qqpei@mail.xidian.edu.cn.

aggregation, thereby decreasing the delay and drop rate due to proximate accesses. On the other hand, multiple rounds of edge aggregations are performed before uploading the updated models to the cloud, aggregating a wider coverage of clients and resulting in a more accurate FL model [19]. Yet, making appropriate resource allocation or client scheduling decisions for HFL is challenging due to the complex communication and learning mechanism of HFL [20], [21].

This paper presents a new framework to comprehensively optimize client scheduling (i.e., client selection and association) and resource allocation (including energy, computation, and communication) for HFL. We consider the clients equipped with rechargeable batteries and relying on the renewable energy harvested from their environment to power local model training and uploading, which has never been studied in the literature, e.g., [21]–[37]. A new Deep Deterministic Policy Gradient (DDPG)-based framework, named two-phase DDPG (TP-DDPG), is developed to adjust client scheduling and resource allocation adapting to the time-varying wireless channels and renewable energy arrivals, thereby balancing the learning delay and model accuracy of HFL.

Apart from its new consideration of energy harvesting-powered clients and comprehensiveness of the problem tackled, a key contribution of the TP-DDPG framework is that we interpret the client association and bandwidth allocation as part of the environment. An algorithm, named straggler-aware client association and bandwidth allocation (SCABA), is developed to optimize the client association and bandwidth allocation (in the second phase of each iteration of TP-DDPG). SCABA relies on decisions made by a DDPG agent on client selection, transmit power, and CPU configuration (in the first phase), thereby generating rewards for the DDPG agent. With the unique and optimal solution of SCABA, the DDPG agent can be trained effectively by interacting with the environment through SCABA. The number of decisions the DDPG agent needs to make is substantially reduced. Consequently, the DDPG can converge rapidly and reliably.

The key contributions of this paper are summarized as follows.

- 1) We propose a new energy harvesting-powered HFL system, where clients are equipped with rechargeable batteries of finite capacity and powered by renewable energy sources. The decisions about client scheduling and resource allocation are meticulously optimized, adapting to time-varying channels and renewable energy arrivals. This differs distinctively from the existing works on HFL systems, which have been typically under the prerequisite of persistent power supply for clients.
- 2) We design the new TP-DDPG framework, which comprehensively optimizes client scheduling (i.e., client selection and association) and resource allocation (including CPU frequency, communication bandwidth, and transmit power). Particularly, we divide the optimization decisions into two groups, with a DDPG agent tailored to learn one of the groups, including client selection, transmit power, and CPU configuration.
- 3) We interpret the other group of decisions, including client association and bandwidth allocation, as part of

the environment. The new SCABA algorithm is developed to optimize these decisions based on the decisions of the DDPG, thereby generating rewards for the DDPG to refine its policy.

Extensive experimental results are carried out to assess the proposed TP-DDPG algorithm. With its substantially reduced learnable action space, the TP-DDPG can rapidly converge to effective policies that can shorten the training time of HFL by 39.4% compared to its benchmarks when the required test accuracy of HFL is 0.9 based on the MNIST dataset. TP-DDPG also enables HFL to converge to the highest accuracy of 0.93 on the CIFAR-10 dataset, while the accuracy is lower than 0.9 for all the benchmarks. This two-stage, latency-sensitive FL architecture can be integrated with edge computing infrastructure to perform real-time AI inference and decision-making at the network edge. This is particularly beneficial for applications, where data needs to be processed locally, such as IoT, autonomous vehicles, and augmented reality systems [38].

Several pioneering works have attempted to optimize resource allocation or client scheduling policies for HFL systems [21]–[37]. These studies usually considered a static cloud aggregation process (or global iteration), for which fixed resource allocation and/or client scheduling decisions were made off-line, e.g., using game theory [26], [34], convex approximation [21], [30], [32], and alternating optimization [31]. These studies, in general, cannot adapt to dynamically changing HFL systems with time-varying wireless channels. While deep reinforcement learning (DRL) has the potential to adapt to environmental changes, the existing DRL-based solutions, i.e., [36], [37], were designed to perform client scheduling and resource allocation one-off (or off-line) and would suffer from limited scalability, if employed online, due to a direct collection of all actions in their action spaces and consequently relatively large action spaces. On the other hand, energy harvesting technology is a key enabler of energy-efficient and self-sustainable HFL systems where the clients are powered by constrained batteries, but it has yet to be considered in these HFL systems. The incorporation of energy harvesting-powered clients would also require client scheduling and resource allocation to adapt to changing energy arrivals, in addition to the time-varying wireless channels.

Unlike the existing studies, in this paper, we consider a new HFL system with clients equipped with rechargeable batteries of finite capacity and relying on the renewable energy harvested from their environment to power local model training and uploading. The proposed TP-DDPG algorithm optimizes client scheduling and resource allocation (including bandwidth allocation, and the CPU frequencies and transmit powers of the clients) online during each round of edge aggregation, adapting to the time-varying system environment.

We note that the convergence speed and stability of a reinforcement learning (RL) algorithm depend heavily on the sizes of its action spaces. The larger the action space is, the more difficulty the RL algorithm can have in converging. As a matter of fact, the convergence time could increase exponentially as the action space grows, if it indeed converges. In many other cases, such an RL algorithm may not converge or even diverge. In light of this, the proposed TP-DDPG

algorithm judiciously segments the action space of the problem at hand and interprets one part of the action space as part of the environment for the other part of the action space. As a consequence, the remaining action space that requires the attention of DDPG is substantially reduced, leading to enhanced convergence and reliability. This can be critical to the efficiency and scalability of HFL systems, when the network is large with more clients involved.

The rest of this paper is organized as follows. An overview of the related works is given in Section II. A model of the HFL system is presented in Section III. A formulation of the problem is provided in Section IV. We elaborate on the new TP-DDPG framework in Section V and evaluate it experimentally in Section VI. The paper concludes with Section VII.

II. RELATED WORKS

Since it was proposed in [3], FL has received widespread attention for its capability of collaboratively training a shared ML model in a privacy-preserving manner. FL still faces challenges arising from practical implementation, including energy efficiency, communication efficiency, model accuracy, and the straggler effect [5], [39]. A number of existing works endeavored to address these challenges from different perspectives, typically under the settings of edge- or cloud-based FL, e.g., [6]–[16]. The studies in [8]–[10] improved the energy efficiency of FL without leveraging battery (dis)charging. By optimizing simultaneous communication and computation resource allocation in NOMA and TDMA, Mo and Xu [8] minimized the total energy consumption at edge clients. For FL networks with CPU-GPU platforms, an energy-efficient resource allocation algorithm was proposed in [9], allowing users to assign resources according to their individual needs. Considering heterogeneous computing and power resources, optimal resource allocation was investigated in [10].

Studies were conducted to improve the efficiency of FL's communications [11]–[13]. These works focused on model compression or communications, and resource allocation or client scheduling was not considered. Compressing model information was introduced and exhibited significant improvement in communication efficiency with minimum impact on training accuracy in [11]. To accelerate global model aggregation, a broadband analog aggregation (BAA) scheme was designed to take advantage of multi-access channels' waveform superposition property in [12]. Along this vein, a unit-modulus analog receive beamforming design for multi-antenna systems was proposed in [13].

To improve model accuracy and alleviate the straggler effect, client scheduling strategies were investigated in energy- and/or latency-aware FL systems [6], [7], [14]–[16]. None of these works integrated energy harvesting techniques for computation-intensive clients or considered a holistic optimization of client scheduling, bandwidth allocation, and the CPU frequencies and emission power of the clients. A heuristic greedy algorithm was suggested in [7] to choose the largest number of clients within a predefined timeframe for training. By latency-aware client selection and resource allocation, Yu

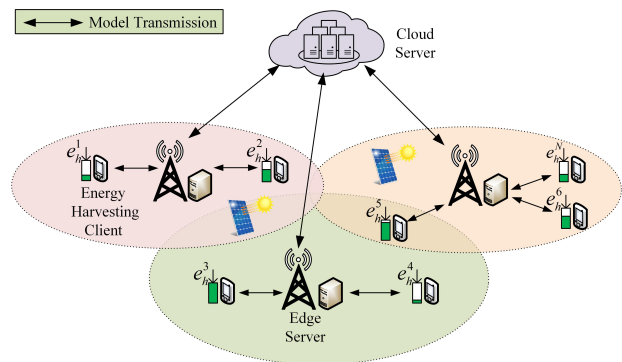


Fig. 1. Illustration of the HFL system.

et al. [14] minimized energy consumption while maximizing selected clients. The impact of different scheduling policies on the performance of FL was studied in [15]. Client scheduling strategies were also investigated considering packet errors [6] and imperfect channel state information [16], respectively.

Recently, several works have attempted to optimize resource allocation and/or client scheduling in HFL systems [21]–[37]. However, the strategies developed in the works are static within a cloud aggregation process, failing to adapt to a dynamically changing environment between different edge aggregations [21]–[33], [36]. Luo *et al.* [21] and Zhang *et al.* [33] collectively optimized the CPU frequency of clients, bandwidth allocation, and client association to effectively reduce the energy consumption and latency of HFL. Feng *et al.* [22] embarked on the cost minimization of individual clients, instead of all clients, and formulated a min-max problem to minimize the worst-case cost of a client. To improve the training performance, Xu *et al.* [23] proposed to select clients with more important local updates, and Qu [24] maximized the number of successful participating clients without dropping out. Deng *et al.* [25] minimized the communication cost by choosing a subset of distributed nodes as the edge aggregator and making decisions on distributed node association. Considering running multiple FL tasks simultaneously, Lim *et al.* [26] developed a framework for resource allocation and incentive mechanism design based on evolutionary game theory. Optimal client associations were also studied to minimize the number of edge-cloud communication rounds [27], loss function [28], Kullback–Leibler divergence (KLD) of data distributions [29], or learning latency [30]. A two-layer algorithm based on genetic algorithm and alternating optimization was proposed to minimize the weighted sum of the optimality gap and overall latency in [31]. A joint helper scheduling and wireless resource allocation scheme was proposed in [32] to capture the importance of weighted gradient. Dynamic resource allocation was studied in [34], [35], [37], which however overlooked the energy consumption or latency of training.

III. SYSTEM MODEL

A. HFL Framework

The considered HFL system comprises a cloud server, a set of edge servers $\mathcal{K} := \{1, \dots, K\}$ co-located with K

TABLE I
NOTATION AND DEFINITION

Notation	Definition
\mathcal{K}	Set of edge servers
\mathcal{N}	Set of clients
\mathcal{D}_n	Client n 's training data set
α_n^t	Selection decision of client n
U	Utility function
$p_n^{t,com}$	Transmission power of client n
$\bar{\omega}_k^{t-1}$	Edge model aggregated by edge server k at the t -th edge aggregation
ω_n^i	Local model of client n at the i -th local iteration
$\bar{\omega}^m$	Global model aggregated by the cloud at the m -th cloud aggregation
R	Number of cloud aggregation rounds of an FL task
R_1	Number of edge aggregation rounds in one cloud aggregation
R_2	Number of local iterations in one edge aggregation
Ω^t	Set of clients selected in the t -th edge aggregation round
\mathcal{Z}_k^t	Set of clients associated with edge server k
f_n^t	CPU frequency of client n for local training
b_{nk}^t	Ratio of bandwidth allocated to client n from edge server k
$T_n^{t,com}, E_n^{t,com}$	Communication delay and energy respectively for client n to upload local model
$T_n^{t,cmp}, E_n^{t,cmp}$	Computation delay and energy respectively of R_2 local iterations of client n
T_g	Total latency of edge model upload and global model aggregation and sharing
T_k^t	Total latency of edge server k in the t -th edge aggregation round
T^t	Latency of completing the t -th edge aggregation across all edge servers
E_n^t	Battery energy level of client n at the beginning of the t -th edge aggregation round
$E_{n,c}^t$	Battery energy level of client n at the end of "on" time
T_c^m	Delay of the m -th cloud aggregation
$E_{n,ho}^t, E_{n,ho}^t$	Harvested energy during "on" time and "idle" time respectively
U_n	Importance of the local model of client n
$\tau_{n,t}$	Latest edge aggregation round when client n was selected before the current t -th round
F	Maximum number of edge aggregation rounds between two consecutive selections of a client

base stations (BSs), and a set of clients $\mathcal{N} := \{1, \dots, N\}$ powered by renewable energy sources, as illustrated in Fig. 1. $N \geq K$. Each client $n \in \mathcal{N}$ has a local dataset \mathcal{D}_n with $|\mathcal{D}_n|$ data samples, where $|\cdot|$ stands for cardinality. For each dataset $\mathcal{D}_n = \{x_{n,d}, y_{n,d}\}_{d=1}^{|\mathcal{D}_n|}$, $x_{n,d}$ is the d -th input data at client n , and $y_{n,d}$ is the corresponding label. Let ω be the parameters of the global FL model, and $f(\omega, x_{n,d}, y_{n,d})$ be the loss function of the FL with the input $x_{n,d}$ and the labeled output $y_{n,d}$. The local loss function of client n is $F_n(\omega) = \frac{1}{|\mathcal{D}_n|} \sum_{d=1}^{|\mathcal{D}_n|} f(\omega, x_{n,d}, y_{n,d})$. The objective of training the global FL model is to minimize the following global loss function, i.e.,

$$F(\omega) = \frac{1}{|\mathcal{D}|} \sum_{n=1}^N |\mathcal{D}_n| F_n(\omega), \quad (1)$$

where $\mathcal{D} = \bigcup_{n \in \mathcal{N}} \mathcal{D}_n$ collects all data samples of all clients.

To minimize $F(\omega)$ in (1) without sharing datasets among the clients and servers, the HFL system adopts an iterative learning protocol. We assume that a total of R rounds of cloud aggregations (i.e., at the cloud server) are required to complete an FL task. Suppose that $\bar{\omega}^0$ is a randomly initialized global model. At the beginning of the m -th cloud aggregation round, $m \in [1, R]$, the cloud server sends the global model $\bar{\omega}^{m-1}$ to all edge servers. Then, the HFL system proceeds with R_1 rounds of edge aggregations (i.e., at the edge servers) before a cloud aggregation is carried out at the server.

In the t -th edge aggregation round that is between the $(m-1)$ -th and the m -th cloud aggregations, i.e., $t \in [(m-1)R_1 + 1, mR_1]$, the cloud server first requests system information and makes resource allocation and client scheduling decisions. Based on these decisions, each edge server $k \in \mathcal{K}$ broadcasts its model $\bar{\omega}_k^{t-1}$ through its associated base station to its clients $n \in \mathcal{Z}_k^t$, where \mathcal{Z}_k^t is the set of clients associated with edge server k in the t -th edge aggregation round. Clearly, $\bar{\omega}_k^{t-1} = \bar{\omega}^{m-1}$ if $t = (m-1)R_1 + 1$. At any moment, an active client can associate with only an edge server, i.e.,

$$\mathcal{Z}_i^t \cap \mathcal{Z}_k^t = \emptyset, \quad i \neq k \text{ and } i, k \in \mathcal{K}. \quad (2)$$

The set of clients selected in the t -th edge aggregation round is $\Omega^t = \bigcup_{k \in \mathcal{K}} \mathcal{Z}_k^t$. Let a binary decision variable α_n^t indicate whether client n is selected to be active in the t -th edge aggregation round. $\alpha_n^t = 1$, if $n \in \Omega^t$; $\alpha_n^t = 0$, otherwise.

Upon receiving an edge model, client n starts to update its local model for R_2 rounds. At the i -th local iteration that is within the t -th edge aggregation round, i.e., $i \in [(t-1)R_2 + 1, tR_2]$, client n performs its local update:

$$\omega_n^i = \omega_n^{i-1} - \eta \nabla F_n(\omega_n^{i-1}), \quad (3)$$

where η is the learning rate and $\nabla F_n(\omega_n^{i-1})$ is the gradient of $F_n(\omega_n^{i-1})$. Clearly, $\omega_n^{i-1} = \bar{\omega}_k^{t-1}$ if $i = (t-1)R_2 + 1$.

After the local update, an orthogonal frequency division multiple access (OFDMA) protocol is employed for the selected clients to upload their local models with a typical size of $10^4 \sim 10^{12}$ bits [40]. Each edge server provides a bandwidth of B to its selected clients. Edge server k receives and averages the updated model parameters $\{\omega_n^{tR_2}, \forall n \in \mathcal{Z}_k^t\}$ from its associated clients.

Consider an importance-oriented weighting proposed in [41] for model aggregation, e.g., to improve model convergence performance when the clients have heterogeneous data distributions. The importance weights can be calculated at the clients based on locally available information, i.e., the edge model of the $(t-1)$ -th round $\bar{\omega}_k^{t-1}$, and the local dataset $\mathcal{D}_n = \{x_{n,d}, y_{n,d}\}_{d=1}^{|\mathcal{D}_n|}$, as given by [31, eq.(1)]

$$U_n = |\mathcal{D}_n| \sqrt{\frac{1}{|\mathcal{D}_n|} \sum_{d \in \mathcal{D}_n} f(\bar{\omega}_k^{t-1}, x_{n,d}, y_{n,d})^2}. \quad (4)$$

The aggregated edge model is given by

$$\bar{\omega}_k^t = \frac{\sum_{n \in \mathcal{Z}_k^t} U_n \omega_n^{tR_2}}{\sum_{n \in \mathcal{Z}_k^t} U_n}. \quad (5)$$

It is worth mentioning that the algorithm proposed in this paper is not limited to a particular scheme, and can apply to other aggregation methods, e.g., the sample number-based weighting [21]¹.

When $t = mR_1$, all edge servers deliver their updated edge models $\{\bar{\omega}_k^{mR_1}, \forall k\}$ to the cloud server for the m -th global model aggregation, i.e.,

$$\bar{\omega}^m = \frac{\sum_{k \in \mathcal{K}} D_k^m \bar{\omega}_k^{mR_1}}{\sum_{k \in \mathcal{K}} D_k^m}, \quad (6)$$

where $D_k^m = \sum_{t=(m-1)R_1+1}^{mR_1} |\mathcal{D}_k^t|$ and $\mathcal{D}_k^t = \bigcup_{n \in \mathcal{Z}_k^t} \mathcal{D}_n$. This concludes a cloud aggregation round and repeats until the global model parameter $\bar{\omega}^m$ meets an accuracy requirement.

The proposed HFL framework works in a synchronous fashion, as it requires all edge servers to commence edge model aggregation only after receiving the local models from all its associated clients, and the cloud server to commence global model aggregation only after receiving the edge models from all edge servers. Synchronous FL has the advantage of ensuring that the global model is updated with the most recent information from the clients before aggregation, generally leading to fewer aggregation rounds and better convergence of the global training [43]. This helps avoid the stale model problem where slow clients may use outdated local models. Synchronous FL is suitable for network infrastructures synchronized, maintained, and operated closely by a network operator, such as the edge networks considered in this paper. The widely adopted network time protocol (NTP) can provide the required synchronization [44]. Specifically, an epoch of local training could last for seconds or even minutes at individual clients. By contrast, the network synchronization protocols, such as NTP, synchronize network devices typically within milliseconds [44]. The required synchronization of model training and aggregation can be achieved by evaluating the processing speed of individual clients or edge servers, and selecting the slowest to specify the durations of aggregation rounds.

On the other hand, distinctively different from synchronous FL [21] and FL with so-called flexible aggregation [45], the aggregations in asynchronous FL start once an edge (or cloud) server receives a prespecified number of local (or edge) models, instead of all local (or edge) models. The formulation and resource allocation of asynchronous FL are substantially different from synchronous FL and beyond the scope of this paper.

B. Computation Model

Local updates can be performed using stochastic gradient descent (SGD). A client randomly selects M samples from the local training data for its local update. Let c_n denote the required CPU cycles to process a bit of data at client n . Suppose that all samples are of the same size, β (in

¹Poisoning attacks on FL (including model poisoning and data poisoning) and defense mechanisms, such as model analysis, Byzantine robust aggregation, and verification-based methods, have been studied [42], which are beyond the scope of this paper.

bits). During a local iteration, the CPU consumes $c_n M \beta$ CPU Cycles at client n .

Let $f_n^t \in [0, f_n^{\max}]$ denote the CPU frequency assigned to the local model training at client n before the t -th edge aggregation. The total CPU frequency assigned to client n should not be larger than f_n^{\max} . The computation latency for client n to perform R_2 rounds of local model updates can be expressed as:

$$T_n^{t,cmp} = \alpha_n^t \frac{R_2 c_n M \beta}{f_n^t}. \quad (7)$$

The energy consumption of the local model updates during $T_n^{t,cmp}$ is [9]:

$$E_n^{t,cmp} = p_n^{t,cmp} T_n^{t,cmp}, \quad (8)$$

where $p_n^{t,cmp} = u_n (f_n^t)^3$ is the power consumption of local computing at client n , and u_n is a constant depending on the effective capacitance coefficient of its computing chipset.

C. Communication Model

Suppose that client n is associated with edge server k in the t -th edge aggregation round. Let $b_{nk}^t \in [0, 1]$ denote the proportion of the edge server's bandwidth allocated to client n at the round, and $p_n^{t,com} \in [0, p_n^{\max}]$ denote the transmission power of client n . According to Shannon's theorem, the achievable transmit rate of client n is given by

$$r_{nk}^t = b_{nk}^t B \log_2 \left(1 + \frac{p_n^{t,com} h_{nk}^t}{\psi^t} \right), \quad (9)$$

where ψ^t is the receiver noise power of the BS, and $h_{nk}^t \in \mathcal{R}^+$ is the channel gain from client n to edge server k . \mathcal{R}^+ denotes the set of positive real values. Since different edge servers (more explicitly, their associated BSs) operate at different, non-overlapping channels and the OFDMA protocol is adopted by the selected clients in each of the channels, there is no interference between the edge servers and between the clients in the uplink.

Let ζ denote the size of the local models produced by the clients. The communication delay for uploading $\omega_n^{tR_2}$ from client n to edge server k is given by

$$T_n^{t,com} = \alpha_n^t \frac{\zeta}{r_{nk}^t}. \quad (10)$$

The energy cost for uploading $\omega_n^{tR_2}$ from client n is:

$$E_n^{t,com} = p_n^{t,com} T_n^{t,com}. \quad (11)$$

Under a synchronous FL framework, the total latency of edge server k in the t -th edge aggregation round depends on the slowest client under the edge server and is given by

$$T_k^t = \max_{n \in \mathcal{Z}_k^t} (T_n^{t,cmp} + T_n^{t,com} + T_e), \quad (12)$$

where T_e is a constant accounting for the downlink model sharing and the model aggregation of the edge servers [21].

The $(t+1)$ -th edge aggregation round does not start until all edge servers complete their t -th edge aggregations. This is because the client association and resource allocation may

change between edge aggregation rounds. The latency of the t -th edge aggregation round is thus given by:

$$T^t = \max_{k \in \mathcal{K}} T_k^t. \quad (13)$$

When $t = mR_1$, the cloud collects the updated models from all edge servers and combines them into a global model. The delay of the m -th cloud aggregation is

$$T_c^m = \sum_{t=(m-1)R_1+1}^{mR_1} T^t + T_g, \quad (14)$$

Here, $T_g = T_u + T_c$. In particular, T_u accounts for the constant latency for the edge servers to transmit their aggregated models to the cloud server; T_c contains the constant model aggregation delay and global model sharing delay of the cloud server [29].

D. Energy Harvesting and Battery Models

The clients each have a rechargeable battery with a capacity of E^{\max} , and are powered by renewable energy. Let E_n^t indicate the battery charging level of client n when the t -th edge aggregation round starts; E_n^1 is the initial battery energy level of client n .

We divide the t -th edge aggregation round into: i) an *on* time from 0 to $T_n^{t,cmp} + T_n^{t,com}$, and ii) an *idle* time from $T_n^{t,cmp} + T_n^{t,com}$ to T^t ; see Fig. 2. A client keeps harvesting energy during both the “on” and “idle” times. The energy harvesting process follows a Poisson distribution with different means $e_n^h \in [e_h^{\min}, e_h^{\max}]$ at different clients. The amounts of energy harvested during the “on” time and the “idle” time are $E_{n,ho}^t$ and $E_{n,hi}^t$, respectively.

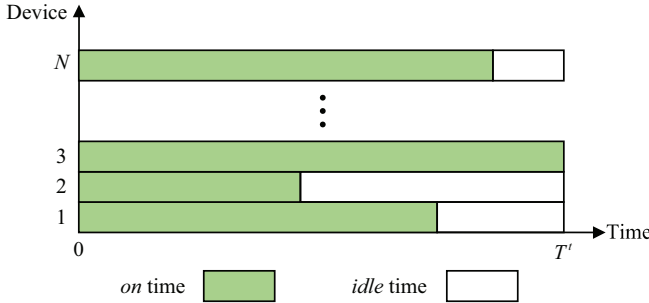


Fig. 2. The time interval of the t -th edge aggregation.

Then, the battery energy level of client n at time $T_n^{t,cmp} + T_n^{t,com}$ is

$$E_{n,c}^t = \min\{E_n^t + E_{n,ho}^t - E_n^{t,cmp} - E_n^{t,com}, E^{\max}\}, \quad (15)$$

where $E_n^t + E_{n,ho}^t \geq E_n^{t,cmp} + E_n^{t,com}$ ensures that the energy initially stored in the battery and collected during the “on” time should be larger than the energy consumption over the “on” time. When the $(t+1)$ -th edge aggregation round starts, the battery level amounts to:

$$E_n^{t+1} = \min\{E_{n,c}^t + E_{n,hi}^t + E_g^t, E^{\max}\}, \quad (16)$$

where E_g^t denotes the harvested energy from time T^t to $(T^t + T_g)$, if a cloud model aggregation occurs after the t -th edge aggregation round; or $E_g^t = 0$, otherwise.

IV. PROBLEM FORMULATION

To accomplish an FL task with a reasonable learning delay and model accuracy, we optimize resource allocation and client schedule in this section. Given the total number of local iterations of an FL task (i.e., $I := RR_1R_2$) and fixed dataset size, $|\mathcal{D}_n|, \forall n$, we can show that the expected global gradient deviation is upper bounded by

$$\begin{aligned} \frac{1}{I} \sum_{i=1}^I \mathbb{E} \|\nabla F(\bar{\omega}^{m_i})\|^2 &\leq \frac{2}{I\eta} [F(\bar{\omega}^1) - F(\bar{\omega}^*)] + \\ \frac{1}{I} \sum_{i=1}^I \sum_{\forall k} \sum_{\forall n} &\left[\Gamma_{k,n}(R_1, R_2) \mathbb{E} (|\mathcal{D}_n| - \alpha_n^{t_i} |\mathcal{D}_n|) + \Psi_{k,n}(R_1, R_2) \right], \end{aligned} \quad (17)$$

where $m_i = \lceil \frac{i}{R_1 R_2} \rceil$, $t_i = \lceil \frac{i}{R_2} \rceil$, $\bar{\omega}^*$ is the optimal global model, $\Gamma_{k,n}(R_1, R_2)$ and $\Psi_{k,n}(R_1, R_2)$ are two increasing functions of R_1 and R_2 . The convergence upper bound in (17) is obtained by extending the analysis presented in [46, Theorem 2]. In particular, persistent client association was considered throughout an HFL process in [46, Theorem 2]. In this paper, we extrapolate that analysis by considering the situation in which the clients may be associated with different edge servers at different edge aggregation rounds.

The upper bound of the expected global gradient deviation on the right-hand side (RHS) of (17) decreases with an increasing number of participating clients, $|\Omega^t| := \sum_n \alpha_n^t$, and increases with the numbers of local iterations in edge and global aggregations, R_2 and $R_1 R_2$. Given R , R_1 , and R_2 , minimizing the upper bound can be transformed equivalently to maximize the number of participating clients $|\Omega^t|$ in each round, since the upper bound decreases with the increasing number of participating clients. On the other hand, scheduling more clients may incur a severer straggler effect and slow the FL process down, especially when there are limited communication and computation resources. We set $O_t = \lambda |\Omega^t| - T^t$ to be the objective function in the t -th edge aggregation round to jointly assess the model accuracy and learning delay of HFL, where λ is a positive control parameter that balances the number of scheduled clients and learning delay.

Since completing an FL task requires R rounds of cloud aggregation, RR_1 rounds of edge aggregation, and RR_1R_2 rounds of local iterations, the overall learning delay is $\sum_{t=1}^{RR_1} T^t + RT_g$, where $T^t = \max_k \{ \max_{n \in \mathcal{Z}_k^t} (\alpha_n^t \frac{R_2 c_n M \beta}{f_n^t} + \alpha_n^t \frac{c}{r_n^t} + T_e) \}$. We aim to maximize the utility function $U := \sum_{t=1}^{RR_1} O_t - RT_g$ by jointly optimizing the client selection α_n^t , client association \mathcal{Z}_k^t , bandwidth allocation b_{nk}^t , and the CPU frequencies and transmit powers of the clients, f_n^t and $p_n^{t,com}$. Since the objective is to maximize the number of scheduled clients and minimize the learning delay of an HFL process, the system tends to select clients in good channel conditions. As a consequence, some clients remaining in poor channel conditions may never be selected. However, these clients may have datasets critical for the model accuracy, especially when heterogeneous data is considered among the clients. To avoid this, we define F to be the maximum number of edge aggregation rounds between two consecutive selections of a client, i.e., $\alpha_n^t = 1$ if $t - \tau_{n,t} = F$, where $\tau_{n,t}$ indicates the latest edge aggregation round when client n was selected before the current t -th round.

Let $\mathbf{A}_t = \{\alpha_n^t, f_n^t, p_n^{t,com}, \mathcal{Z}_k^t, b_{nk}^t \mid n \in \mathcal{N}, k \in \mathcal{K}\}$ collect the optimization variables. The problem considered is

$$\max_{\mathbf{A}_t} U = \sum_{t=1}^{RR_1} O_t - RT_g \quad (18a)$$

$$\text{s.t. } E_n^t + E_{n,ho}^t \geq E_n^{t,cmp} + E_n^{t,com}, \quad \forall n, t, \quad (18b)$$

$$E_{n,c}^t = \min\{E_n^t + E_{n,ho}^t - E_n^{t,cmp} - E_n^{t,com}, E^{\max}\}, \quad (18c)$$

$$E_n^{t+1} = \min\{E_{n,c}^t + E_{n,hi}^t + E_g^t, E^{\max}\}, \quad (18d)$$

$$\alpha_n^t = \{0, 1\}, \quad \forall n, t, \quad (18e)$$

$$\sum_{n \in \mathcal{Z}_k^t} b_{nk}^t = 1, \quad b_{nk}^t \in [0, 1], \quad \forall k, t, \quad (18f)$$

$$\alpha_n^t = 1, \text{ if } t - \tau_n^t = F, \quad \forall n, t, \quad (18g)$$

$$0 \leq p_n^{t,com} \leq p_n^{\max}, \quad \forall t, n \in \Omega^t, \quad (18h)$$

$$0 \leq f_n^t \leq f_n^{\max}, \quad \forall t, n \in \Omega^t, \quad (18i)$$

$$\mathcal{Z}_i^t \cap \mathcal{Z}_k^t = \emptyset, \quad \forall t, i \neq k, i, k \in \mathcal{K}. \quad (18j)$$

Constraints (18b)–(18d) ensure the energy causality. (18e) and (18f) provide the feasibility conditions of client selection and bandwidth allocation, respectively. (18h) and (18i) specify the feasible regions of the CPU frequencies and transmit powers of the clients, respectively. (18j) ensures each selected client is associated with only one edge server.

As shown in (18b), energy harvesting affects the available energy in the battery E_n^t , and the latter further constrains the energy consumption of local computing $E_n^{t,cmp}(\alpha_n^t, p_n^{t,com})$ and local model uploading $E_n^{t,com}(\alpha_n^t, f_n^t)$ at the clients. As a consequence, the decisions of the client selection α_n^t , as well as the CPU frequencies and transmit powers of the clients, f_n^t and $p_n^{t,com}$, all depend on the energy harvesting. On the other hand, more participating clients (i.e., larger $|\Omega^t| = \sum_n \alpha_n^t$) can help improve the model accuracy. Meanwhile, larger f_n^t and $p_n^{t,com}$ can shorten the training delay, given the computation latency $T_n^{t,cmp} = \alpha_n^t \frac{R_2 c_n M \beta}{f_n^t}$ and the communication latency $T_n^{t,com} = \alpha_n^t \frac{\zeta}{r_{nk}^t (p_n^{t,com})}$. To this end, energy harvesting, model accuracy, and training delay are highly interdependent.

It is challenging to solve problem (18) directly. First, obtaining the optimal solution to problem (18) would require the perfect *a-priori* knowledge of the system (including channel conditions and energy arrival rates) throughout the HFL process, which is impossible in practice. Even if the *a-priori* knowledge were available, problem (18) would still be an intractable mixed-integer nonlinear programming problem (MINLP) that is typically NP-hard. Further, the evolution of the battery energy level in (18c) and (18d) leads to the coupling of the optimization variables over time. Specifically, the resource allocation and client scheduling in the past can affect the current battery energy level and, in turn, the current resource and client scheduling decisions. For example, if high CPU frequencies or transmit powers are nearsightedly decided to maximize the current O_t in the t -th edge aggregation round, there is no other option but to take low CPU frequencies and transmit powers for a lower O_{t+1} in the $(t+1)$ -th edge aggregation round due to insufficient energy in the battery.

V. PROPOSED TP-DDPG SCHEME

As problem (18) entails a Markov decision process (MDP), we resort to DDPG, the state-of-the-art DRL technique for learning effective decisions in complex and dynamic environments. However, direct use of DDPG to solve problem (18) may not converge, since, as the numbers of clients and edge servers grow, the MDP is increasingly complex with the number of variables in \mathbf{A}_t . In this section, we delineate the new TP-DDPG framework to solve problem (18) with a significantly improved convergence rate. In the first phase, the selection of participating clients, transmit powers, and CPU configurations are decided by the DDPG for each edge aggregation round. In the second phase, the rest of problem (18) is efficiently solved using the new SCABA, which is interpreted as part of the environment for the DDPG and produces rewards for the DDPG agent for model training.

A. Discrete-Time MDP Framework for RL

Being an MDP, problem (18) can be characterized using a 3-tuple $(\mathcal{S}, \mathcal{A}, \mathbf{r})$, where \mathcal{S} , \mathcal{A} , and \mathbf{r} are the state, action, and reward of the MDP, respectively.

1) **State \mathcal{S}** : In the t -th edge aggregation round, the system state $\mathbf{s}_t \in \mathcal{S}$ is defined to be $\mathbf{s}_t = \{E_{n,c}^{t-1}, E_n^t, h_{nk}^t, \tau_n^t, \forall n \in \mathcal{N}, \forall k \in \mathcal{K}\}$. Recall that $E_{n,c}^{t-1}$ is the battery energy level of client n at the end of the *on* time in the $(t-1)$ -th edge aggregation round; E_n^t is the battery charging level of client n when the t -th edge aggregation round begins; h_{nk}^t is the channel gain from client n to edge server k in the t -th edge aggregation round; and τ_n^t indicates the latest edge aggregation round when client n was selected before the current t -th round.

2) **Action \mathcal{A}** : To reduce the action space and accelerate convergence, we design the action of the DDPG model in the t -th edge aggregation round to be $\mathbf{a}_t = \{\alpha_n^t, f_n^t, p_n^{t,com}, \forall n\} \in \mathcal{A}$. Here, α_n^t is the binary client selection decision; f_n^t and $p_n^{t,com}$ are the CPU frequency and transmit power of client n , respectively, if the client is selected.

3) **Reward \mathbf{r}** : A reward evaluates the action executed. For problem (18), a straightforward design principle would set the instantaneous objective function in (18a), i.e., O_t , as the immediate reward. In contrast, we define the reward to be an exponential function of the instantaneous objective, i.e.,

$$r_t = e^{(c+O_t)} - \varphi, \quad (19)$$

where c is a tunable parameter, and φ is the penalty if constraints (18b) and (18g) are unsatisfied. The immediate reward (19) is produced by a new straggler-aware client association and bandwidth allocation algorithm, given the action $\mathbf{a}_t = \{\alpha_n^t, f_n^t, p_n^{t,com}, \forall n\}$ taken by the DDPG.

B. Proposed DDPG-Based Client Selection, Power Control and CPU Configuration

At any edge aggregation round t , the DDPG agent deployed at the cloud server perceives the state \mathbf{s}_t and executes action \mathbf{a}_t . After executing the action, the environment feeds back a scalar reward r_t and transfers from state \mathbf{s}_t to \mathbf{s}_{t+1} . Let $\pi(\mathbf{s}_t)$ denote the policy that projects state \mathbf{s}_t to action \mathbf{a}_t .

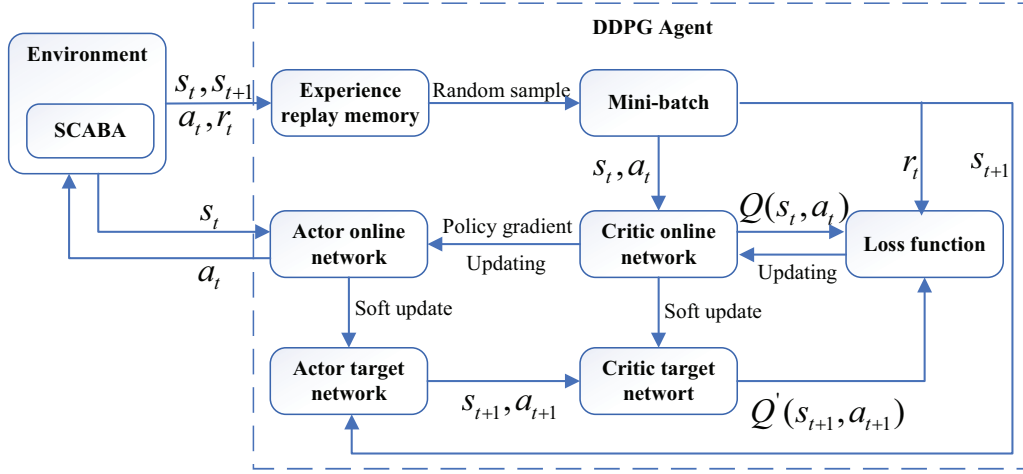


Fig. 3. The structure of the proposed TP-DDPG algorithm, where a DDPG agent consisting of actor-critic networks and an experience replay memory makes decisions on client selection, power control and CPU configuration, and the SCABA decides on client association and bandwidth allocation. The SCABA can be interpreted as part of the environment for the DDPG, and produces a reward for each decision that the DDPG agent makes on client selection, transmit power, and CPU configuration.

Let $Q^\pi(s, \mathbf{a})$ denote the action-value function that represents the expected accumulative discounted reward over infinite time under the policy π with the initial state s and the initial action \mathbf{a} , as given by:

$$Q^\pi(s, \mathbf{a}) = \mathbb{E}_\pi \left[\sum_{i=0}^{\infty} \gamma^i r_{t+i} | s_t = s, \mathbf{a}_t = \mathbf{a} \right], \quad (20)$$

where $\gamma \in [0, 1]$ denotes the discount factor.

The agent aims to learn the optimal policy $\pi^*(s)$:

$$\pi^*(s) = \arg \max_{\mathbf{a}} Q^*(s, \mathbf{a}), \quad (21)$$

where $Q^*(s, \mathbf{a}) = \max_{\pi} Q^\pi(s, \mathbf{a})$ is the optimal action-value function. Among many DRL algorithms, DDPG is suited for our considered problem because of its capability to cope with the continuous state and action spaces. With the actor-critic framework, the DDPG model applies the actor-network to fit the policy π , and the critic network to approximate the action-value function $Q^\pi(s, \mathbf{a})$. An actor network or critic network contains two sub-networks with the same architecture: a target network and an online network. This ensures learning stability and prevents overestimation in large-scale problems.

Let $\pi(s_t | \theta^\pi)$ and $Q(s_t, \mathbf{a}_t | \theta^Q)$ denote the actor and critic online networks, respectively; θ^π and θ^Q are the model parameters of the two deep neural networks (DNNs). Let $\pi'(s_t | \theta^{\pi'})$ and $Q'(s_t, \mathbf{a}_t | \theta^{Q'})$ denote the actor and critic target networks, respectively; $\theta^{\pi'}$ and $\theta^{Q'}$ are the model parameters of the two DNNs. In order to update the critic online network, the following loss function is minimized:

$$L(\theta^Q) = \frac{1}{M'} \sum_t [(y_t - Q(s_t, \pi(s_t | \theta^\pi) | \theta^Q))^2], \quad (22)$$

where $y_t = r_t + \gamma Q'(s_{t+1}, \pi'(s_{t+1} | \theta^{\pi'}) | \theta^{Q'})$ and M' is the size of a mini-batch. We optimize the actor online network in the direction of $\nabla_{\theta^\pi} J(\theta^\pi) \approx$

$\frac{1}{M'} \sum_t \nabla_{\mathbf{a}_t} Q(s_t, \mathbf{a}_t | \theta^Q) \nabla_{\theta^\pi} \pi(s_t | \theta^\pi)$ to maximize the following policy objective function:

$$J(\theta^\pi) = \mathbb{E}_{\theta^\pi} [Q(s_t, \pi(s_t | \theta^\pi) | \theta^Q)], \quad (23)$$

where ∇_{θ^π} denotes the derivative w.r.t θ^π . Then, the actor and critic target networks are updated softly by

$$\theta^{\pi'} \leftarrow \phi \theta^\pi + (1 - \phi) \theta^{\pi'}; \quad (24)$$

$$\theta^{Q'} \leftarrow \phi \theta^Q + (1 - \phi) \theta^{Q'}, \quad (25)$$

where ϕ is a parameter controlling the learning speed.

The proposed TP-DDPG algorithm is depicted in Fig. 3, and summarized in Algorithm 1. In each edge aggregation round, the DDPG agent collects necessary state information s_t from the environment. The clients and the edge servers upload their local observations, together with their trained models. The cloud server sends back its decisions on the actions, along with the global model. The latency and energy consumption of transmitting the states and actions are comparatively negligible, since their size is negligible compared to the model size. The actor online network outputs action \mathbf{a}_t . Given \mathbf{a}_t , we optimize the remaining decisions $\{z_k^t, b_{nk}^t, \forall n, k\}$ to evaluate the reward, as will be articulated in Section V-C. The agent obtains the reward r_t at the end of edge aggregation t and observes a new state s_{t+1} .

An experience replay pool is added to the DDPG agent to preserve the experience $\{s_t, \mathbf{a}_t, r_t, s_{t+1}\}$ in each iteration. The learning process commences when the experience replay buffer is full. Specifically, a mini-batch of M' experiences is obtained by randomly sampling the replay buffer to train the DDPG network. The critic and actor online networks are then updated by minimizing the loss function in (22) and maximizing the policy objective function in (23), respectively, followed by the update of the target networks via (24) and (25). The model can converge after hundreds of episodes by suppressing the correlations between observations and exploring different environment states.

Algorithm 1: Proposed TP-DDPG Algorithm

```

1 Initialize the actor online network and critic online
  network with random model parameters  $\theta^\pi$  and  $\theta^Q$ ,
  respectively.
2 Initialize the actor target network and critic target
  network with model parameters  $\theta^{\pi'} \leftarrow \theta^\pi$  and
   $\theta^{Q'} \leftarrow \theta^Q$ , respectively.
3 Initialize the experience replay buffer with size  $V$ .
4 Parameter updating:
5 for each episode do
6   Initialize the environment and receive the initial
     observed system state  $s_1$ .
7   for edge aggregation round  $t = 1, 2, \dots, RR_1$  do
8     Choose action  $\mathbf{a}_t = \pi(\mathbf{s}_t|\theta^\pi) + N_0$  via the actor
       online network with the exploration noise  $N_0$ .
9     Given  $\mathbf{a}_t$ , obtain the client association and
       bandwidth allocation strategy by using
       Algorithm 2.
10    Obtain reward  $r_t$  and the subsequent state  $s_{t+1}$ .
11    Save experience  $\{s_t, \mathbf{a}_t, r_t, s_{t+1}\}$  in the replay
       buffer.
12    if the experience replay buffer is full then
13      Randomly sample  $M'$  transitions from the
        buffer and input them to the actor and
        critic networks.
14      Update the critic and actor online networks
        by minimizing (22) and maximizing (23),
        respectively.
15      Update the target networks via (24) and
        (25).
16    end
17  end
18 end

```

C. Straggler-Aware Client Association and Bandwidth Allocation

To mitigate the straggler effect in an edge aggregation round for the considered synchronous FL updates, we propose to use DDPG in the first phase of TP-DDPG to adaptively select clients preferably in good channel conditions in a round and avoid selecting straggling clients. Then, we propose the SCABA in the second phase to identify the straggling edge server in each iteration, hence reducing its latency for edge aggregation. This is done by iteratively adjusting the association and bandwidth allocation strategy until the latency cannot be further shortened. In this way, the straggler effect in a global aggregation round can be significantly alleviated.

Given the action $\mathbf{a}_t = \{\alpha_n^t, f_n^t, p_n^{t,com}, \forall n\}$ taken by the proposed DDPG in the t -th edge aggregation round, problem (18) is reduced to:

$$\min_{\mathcal{Z}_k^t, b_{nk}^t} T^t \quad \text{s.t.} \quad (18b), (18f), (18j), \quad (26)$$

where the number of participating clients $|\Omega^t|$ is suppressed from the original objective function, i.e., $|\Omega^t| = \sum_n \alpha_n^t$.

The client association and bandwidth allocation problem in (26) is to distribute the clients among the edge servers and allocate the bandwidth of the edge servers to the selected clients. The problem is a complex combinatorial optimization problem. In what follows, we decompose problem (26) into client association and bandwidth allocation subproblems, and delineate the SCABA, which balances learning delay and accuracy with low complexity.

First, the SCABA initializes the client association decision $\mathcal{Z}^t = \{\mathcal{Z}_k^t : k \in \mathcal{K}\}$ by connecting each selected client to the edge server with the strongest channel gain. Given \mathcal{Z}_k^t , the bandwidth allocation sub-problem concerning edge server k can be written as

$$\min_{b_{nk}^t} T_k^t \quad (27a)$$

$$\text{s.t.} \quad \sum_{n \in \mathcal{Z}_k^t} b_{nk}^t = 1, \quad b_{nk}^t \in [0, 1], \quad \forall k, t. \quad (27b)$$

Recall $T_k^t = \max_{n \in \mathcal{Z}_k^t} (T_n^{t,cmp} + T_n^{t,com} + T_e)$. By introducing an auxiliary variable T , the problem in (27) is rewritten as

$$\min_{b_{nk}^t} T \quad (28a)$$

$$\text{s.t.} \quad T \geq T_n^{t,cmp} + T_n^{t,com} + T_e, \quad \forall n \in \mathcal{Z}_k^t. \quad (28b)$$

$$\sum_{n \in \mathcal{Z}_k^t} b_{nk}^t = 1, \quad b_{nk}^t \in [0, 1], \quad \forall k, t. \quad (28c)$$

Given the action $\mathbf{a}_t = \{\alpha_n^t, f_n^t, p_n^{t,com}, \forall n\}$, $T_n^{t,cmp}$ and T_e are constants, and $T_n^{t,com}$ is inversely proportional to b_{nk}^t . Since the objective function and the inequality constraint (28b) are convex while the equality constraint (28c) is an affine function, problem (28) is convex and can be solved optimally using convex solvers. We use the off-the-shelf function *fminimax* in Matlab toolkit to solve problem (27). After solving problem (27) for all edge servers for $k \in \mathcal{K}$, we can obtain the minimum edge aggregation delay $T^t = \max_{k \in \mathcal{K}} T_k^t$.

Next, we update the client association \mathcal{Z}^t by moving or swapping the clients associated with the straggler, and then solve problem (27) again until the edge aggregation delay T^t cannot be further reduced. Particularly, we propose to update the client association in the following ways.

- 1) We can obtain a new client association strategy \mathcal{Z}^t by removing client n from $\mathcal{Z}_{v^*}^t$, the set of clients associated with the straggler v^* , to another set \mathcal{Z}_l^t ;
- 2) Or we can pick one client $n \in \mathcal{Z}_{v^*}^t$ and one client $n' \in \mathcal{Z}_l^t$, and swap their association strategy.

A historical straggler set, denoted by \mathcal{H} , is maintained in every edge aggregation round t to record the straggling edge server k and its associated clients \mathcal{Z}_k^t . If a server-client pair (k, \mathcal{Z}_k^t) in a new client association \mathcal{Z}^t satisfies $(k, \mathcal{Z}_k^t) \in \mathcal{H}$, $\exists k \in \mathcal{K}$, we skip \mathcal{Z}^t since its corresponding edge aggregation delay cannot be shorter than the minimum delay under the explored client associations. A straggler is the last edge server required to complete the edge aggregation. It is the bottleneck of edge aggregation. If a client association has caused a straggler problem, it would not be assessed again.

The key idea of the SCABA is to identify the straggling edge server in each iteration, and reduce its latency for completing

edge aggregation by repeatedly adjusting its association and bandwidth allocation strategy until the latency cannot be further shortened. Algorithm 2 summarizes the proposed SCABA, where $\mathcal{B}^t = \{b_{nk}^t | n \in \Omega^t, k \in \mathcal{K}\}$, and $\tilde{\mathcal{T}}^t = \{T_k^t | k \in \mathcal{K}\}$. We first initialize \mathcal{Z}^{t*} by connecting each selected client to the edge server with the strongest channel gain, and obtain \mathcal{B}^{t*} and $\tilde{\mathcal{T}}^{t*}$ by solving problem (27) in Steps 1 and 2. Next, we find the straggling edge server v^* . Then, we iteratively adjust the client association (by switching clients away from the straggler server or swapping the clients with those associated with other servers) to minimize the learning period of the straggler until the delay cannot be shortened or the maximum number of iterations, denoted by ξ , is reached.

In each iteration, only when the edge aggregation delay T_v^t corresponding to the client association \mathcal{Z}^t and bandwidth allocation \mathcal{B}^t is shorter than $T_{v^*}^{t*}$, should the optimal client association and bandwidth allocation decisions be updated, together with the delay and straggler; see Steps 10–13. By switching out or swapping the clients associated with the straggling edge server to shorten the edge aggregation delay, the SCABA can converge to a stable and optimal client association and bandwidth allocation strategy within a limited number of iterations, where each edge server owns a stable set of associated clients to achieve the minimum edge aggregation delay. In other words, the delay cannot be further shortened by further adjusting the client association strategy.

D. Analysis of Computational Complexity

In the first phase of the proposed TP-DDPG framework, the DDPG-based algorithm generates action \mathbf{a}_t . In DNNs, the complexity is dependent on the specification. Suppose that the actor and critic networks have I_a and I_c fully connected layers, respectively. The complexity of the DDPG-based algorithm is $\mathcal{O}(\sum_{i=0}^{I_a-1} v_i^a v_{i+1}^a + \sum_{i=0}^{I_c-1} v_i^c v_{i+1}^c)$, where v_i^a and v_i^c denote the numbers of neurons in the i -th layer of the actor and critic networks, respectively [47].

In the second phase, the SCABA produces the client association and bandwidth allocation with the complexity dominated by iteratively solving (27) under different client association policies. Function $fminmax$ used to solve (27) for edge server k employs a sequential quadratic programming (SQP) method, incurring the complexity of $\mathcal{O}(|\mathcal{Z}_k^t|^3)$ [48]. Hence, solving (27) for all edge servers ($k = 1, \dots, K$) incurs the complexity of $\mathcal{O}(|\Omega^t|^3)$ in the worst-case scenario. Let G denote the number of attempts to adjust the client association. The computational complexity of the SCABA is $\mathcal{O}(G|\Omega^t|^3)$.

The proposed TP-DDPG algorithm offers the advantage of both offline training and online testing. Offline training boasts computational efficiency, quicker convergence, and optimal utilization of available data. Online testing enables the agent to adapt and refine its policy in real-time. Specifically, online testing facilitates continuous improvement of the policy by evaluating its performance and making adjustments on-the-fly based on real-time feedback [49].

Algorithm 2: Proposed SCABA

Input: $\Omega^t, f_n^t, p_n^t, h_{nk}^t$, and $\mathcal{H} = \emptyset, \forall n \in \Omega^t, k \in \mathcal{K}$.
Output: Optimal client association \mathcal{Z}^{t*} , and bandwidth allocation \mathcal{B}^{t*} .

- 1 Connect each selected client $n \in \Omega^t$ to the edge server with the strongest channel gain to initialize \mathcal{Z}^{t*} .
- 2 Given \mathcal{Z}^{t*} , obtain \mathcal{B}^{t*} and $\tilde{\mathcal{T}}^{t*}$ by solving (27).
- 3 Find the straggling edge server $v^* = \arg \max_{k \in \mathcal{K}} \tilde{\mathcal{T}}^{t*}$, and put $(v^*, \mathcal{Z}_{v^*}^{t*})$ into \mathcal{H} .
- 4 **repeat**
- 5 **for** $l \in \mathcal{K}, l \neq v^*$ **do**
- 6 Set $\mathcal{Z}^t = \mathcal{Z}^{t*}$, then randomly pick client $n \in \mathcal{Z}_{v^*}^{t*}$, and transfer client n to \mathcal{Z}_l^t .
- 7 **if** $(k, \mathcal{Z}_k^t) \notin \mathcal{H}, \forall k \in \mathcal{K}$ **then**
- 8 Given \mathcal{Z}^t , obtain \mathcal{B}^t and $\tilde{\mathcal{T}}^t$ by solving (27).
- 9 Set $v = \arg \max_{k \in \mathcal{K}} \tilde{\mathcal{T}}^t$, and put (v, \mathcal{Z}_v^t) into \mathcal{H} .
- 10 **if** $T_{v^*}^{t*} > T_v^t$ **then**
- 11 Set $\mathcal{Z}^{t*} = \mathcal{Z}^t, \mathcal{B}^{t*} = \mathcal{B}^t, \tilde{\mathcal{T}}^{t*} = \tilde{\mathcal{T}}^t$ and $v^* = v$.
- 12 **break.**
- 13 **end**
- 14 **end**
- 15 **end**
- 16 **for** $l \in \mathcal{K}, l \neq v^*$ **do**
- 17 Set $\mathcal{Z}^t = \mathcal{Z}^{t*}$, then randomly pick client $n \in \mathcal{Z}_{v^*}^t$ and $n' \in \mathcal{Z}_l^t$, and swap their association strategy, i.e., let $n \in \mathcal{Z}_l^t$ and $n' \in \mathcal{Z}_{v^*}^t$.
- 18 **end**
- 19 Perform Steps 7-15.
- 20 **until** No shorter delay can be obtained or ξ times of adjustment attempts is reached;
- 21 Return \mathcal{Z}^{t*} and \mathcal{B}^{t*} .

VI. PERFORMANCE EVALUATION

Performance evaluation is provided to demonstrate the effectiveness and merits of our proposed algorithm.

A. Experimental Settings

Consider an HFL system with three edge servers and ten clients uniformly distributed in a circular area with a radius of 250 m. A cloud server situates at the center of the area. Suppose that the channel gain between an edge server and a client yields the path loss model $30 \log(d) + 72.4$ (in dB) and Rayleigh fading, where d (in km) is the distance between the edge server and the client [50]. The channel gain remains unchanged throughout a round of edge aggregation and changes independently between rounds. Suppose that a Poisson distribution governs the renewable energy arrival rate at each client, with the mean uniformly distributed within [200, 1000] mJ. The energy arrival rates change every second. By rigorously testing different values and assessing their

corresponding convergence and performance, we set $c = 5$ and $\varphi = 5000$ for the reward function in (19).

Consider classification FL tasks of handwritten digits using the MNIST dataset with 10 digit labels $\{0, 1, \dots, 9\}$ and a convolutional neural network (CNN) model. Each client is assigned 2000 heterogeneous training samples with two labels, e.g., client 1 owns labels $\{0, 2\}$ and client 2 owns labels $\{6, 7\}$. The total number of cloud aggregations is $R = 150$. In each cloud aggregation, the number of edge aggregation and local updates are 5 and 100, respectively. The other parameter settings are provided in Table II.

TABLE II
PARAMETERS FOR PERFORMANCE ANALYSIS

Parameter	Value
Number of edge servers, K	3
Number of clients, N	10
Bandwidth of an edge server, B	1 MHz
Client transmission power, $p_n^{t,com}$	$[0, 1]$ W
Client CPU frequency, f_n^t	$[0, 3]$ GHz
CPU cycles computing per bit data, c_n	$[30, 100]$
Background noise, ψ	10^{-9} W
Uploaded model size, ζ	0.2 MB
Batch size, M and M'	32
Effective capacitance coefficient, u_n	2×10^{-28}
Discount factor, γ	0.99
The maximum round for not selecting a client, F	3
Times of adjustment attempts, ξ	5
Dataset	MNIST
DDPG memory size	40000
DDPG actor learning rate	0.0001
DDPG critic learning rate	0.0002

No existing works has considered a holistic optimization of client scheduling, bandwidth allocation, and the CPU frequencies and transmission powers of the clients in an energy-harvesting HFL system. With due diligence, we compare the proposed TP-DDPG algorithm against the baselines listed below.

- 1) Greedy Association (GA): Client n is associated with the edge server with the strongest channel gain.
- 2) Even Bandwidth Allocation (EBA): The bandwidth of edge server k is evenly allocated to its associated clients.
- 3) Random Selection (RS): Each edge server randomly selects a fixed number of clients in an edge aggregation round. The number of selected clients is configurable.
- 4) Negative Strategy (NS): The decision variable \mathbf{A}_t remains unchanged during a cloud aggregation and only varies between different cloud aggregations.
- 5) DDPG-Only: All decisions in \mathbf{A}_t are generated using only the DDPG.
- 6) Holistic Optimization (HO): In each round of edge aggregation, a fixed number of clients with the largest energy stored in their batteries are selected and associated with the edge server with the strongest channel gain. Subsequently, the bandwidth allocation, CPU frequency, and transmission power decisions are holistically optimized locally through the off-the-shelf function f_{minimax} in Matlab toolkit.

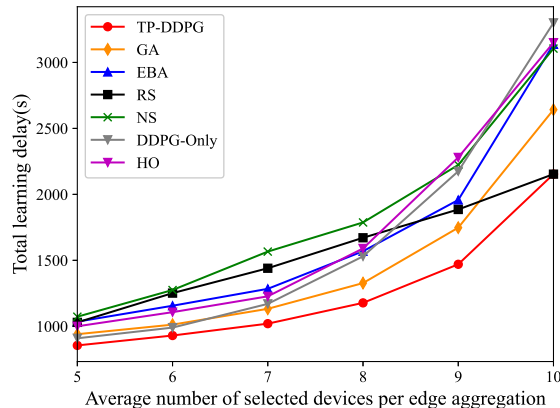


Fig. 4. Learning delay versus the average number of scheduled clients per edge aggregation round.

- 7) Multi-agent deep deterministic policy gradient (MADDPG): To compare the proposed TP-DDPG algorithm with its decentralized counterpart, we design and test the MADDPG, where a DDPG agent is placed at each client, enabling the clients to generate resource allocation and client scheduling decisions in parallel. (No agent can be placed at an individual edge server, since the clients associated with a server can change dynamically.) After each client/agent obtains the client schedule, CPU frequency and transmission power, the edge servers decide the bandwidth allocation under the constraint of the total available bandwidth of an edge server.

B. Numerical Results

Fig. 4 plots the total learning delay versus the average number of selected clients per edge aggregation round under the different schemes. It is shown that as long as the number of selected clients remains the same, the proposed TP-DDPG algorithm always completes its FL task with the shortest latency. The improvement of the TP-DDPG increases as the number of selected clients grows, compared with the NS, BEA, GA, and DDPG-Only algorithms. For instance, as the selected clients increase from five to ten, the additional delay required by the DDPG-Only increases from 6.3% to 53.3%, compared to the TP-DDPG algorithm. When all clients participate in each edge aggregation (i.e., the number of selected clients is 10), the RS is equivalent to the proposed TP-DDPG algorithm and produces the same delay.

Fig. 5 plots the system utility U as the number of episodes grows, to show the convergence of all algorithms. We see that the utilities of all algorithms are relatively small and stable in the first 80 episodes. This is because the parameters of the DDPG models are randomly initialized and would not be updated until the DDPG memory is full. The proposed TP-DDPG algorithm converges to the largest utility within 2500 episodes. In other words, the algorithm can schedule more clients to join the FL task by adaptive client selection and association. In other words, better learning accuracy can be achieved within a shorter delay. We also see that the

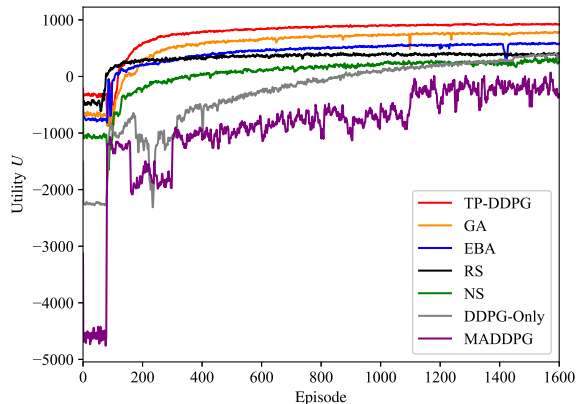


Fig. 5. System utility U as the number of episode grows when $\lambda = 0.35$.

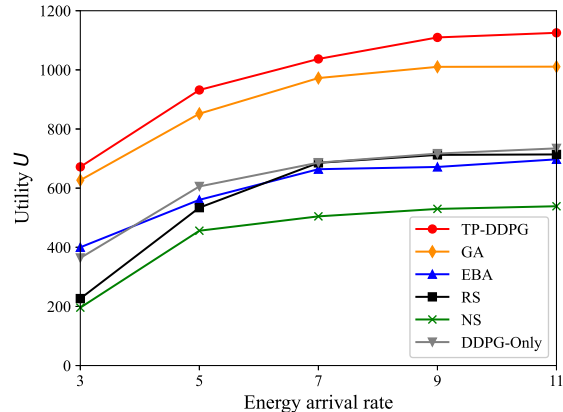


Fig. 7. System utility U versus energy arrival rate.

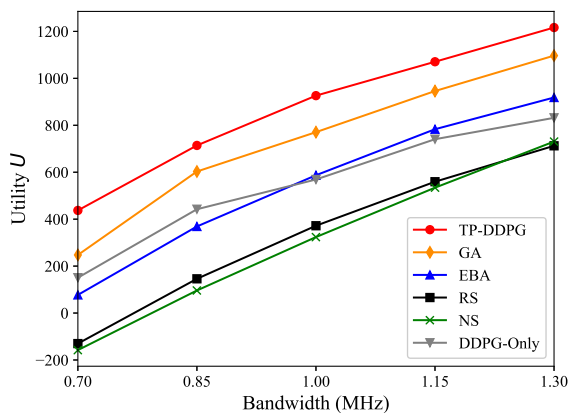


Fig. 6. System utility U versus available Bandwidth.

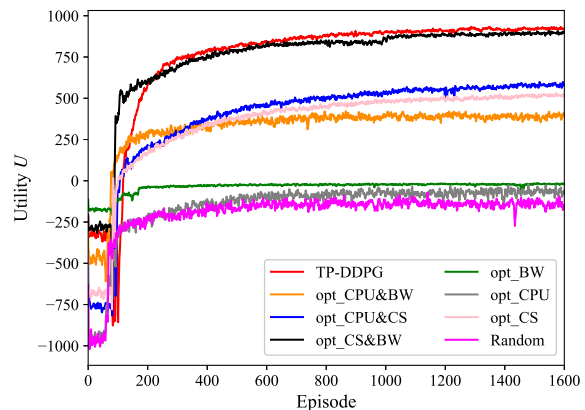


Fig. 8. An ablation study of the system utility U as the number of episodes grows.

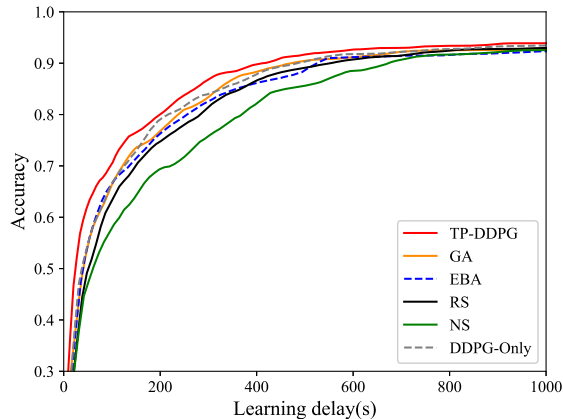
convergence rate of the DDPG-Only is slow due to the large dimension of its state and action spaces.

As shown in Fig. 5, although the state and action spaces are smaller for each DDPG agent, the MADDPG algorithm converges slower to a lower system utility than the proposed TP-DDPG. Furthermore, placing multiple DDPG agents at the clients can result in additional energy consumption of the clients. Despite its centralized training mechanism, the TP-DDPG substantially reduces the state and action spaces and achieves better convergence by introducing the new straggler-aware client association and bandwidth allocation algorithm, i.e., SCABA.

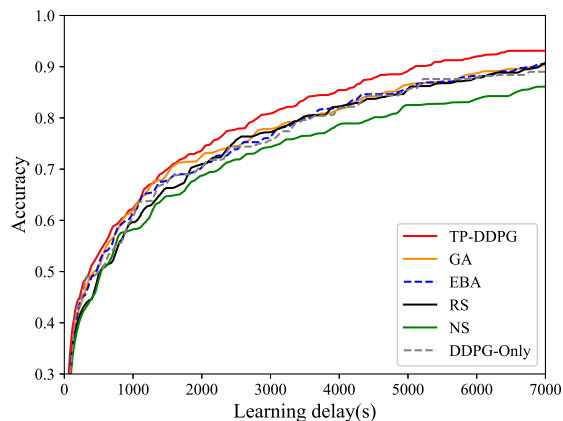
Fig. 6 depicts how the available bandwidth affects the performance of the system. As the bandwidth of the system increases, the system utilities of all algorithms grow. This is because a larger bandwidth leads to a higher transmission rate of local model uploading, thus resulting in a shorter transmission delay. It is noted that the utility gain caused by the increased bandwidth of the DDPG-Only is smaller than that of the TP-DDPG. As the available bandwidth grows, the DDPG-Only faces a larger action space for the bandwidth allocation, thus deteriorating the learning performance.

Fig. 7 shows the system utilities of different algorithms, as the energy arrival rate increases. All schemes show an improvement in system utility when the energy arrival rate increases. The TP-DDPG algorithm always outperforms the benchmarks, as the average energy arrival rate grows from 0.3 W to 1.1 W. With increasing energy arrival rates, the utility U increases slowly and eventually stabilizes. This is because excessively harvested energy would cause the battery to overflow under the limited battery capacity.

An ablation study is conducted to optimize client selection (CS), bandwidth (BW), and CPU frequency separately (as compared to the proposed joint optimization in TP-DDPG), as shown in Fig. 8. It is evident that when only one of the three decisions is optimized while setting the other two randomly, optimizing client selection outperforms optimizing either bandwidth or CPU frequency alone. When two decisions are taken into account, jointly optimizing client selection and bandwidth performs best in improving the utility. While the TP-DDPG outperforms all benchmarks by conducting comprehensive optimization across all three decisions, client selection contributes predominantly to the superiority of the method, followed by bandwidth allocation.



(a) Test accuracy versus learning delay using MNIST.



(b) Test accuracy versus learning delay using CIFAR-10.

Fig. 9. Test accuracy versus learning delay using different datasets.

The test accuracy of the FL models derived under the different algorithms is plotted with respect to the learning delay in Fig. 9(a). The test accuracy is the average of ten independent tests. We see that the proposed TP-DDPG always achieves the highest test accuracy. Given a predefined accuracy, the TP-DDPG significantly shortens the learning time. For instance, the TP-DDPG can save up to 39.4% of the learning time compared to the NS, when the required test accuracy is 0.9. This is because the TP-DDPG changes the resource allocation and client scheduling policy for different edge aggregations, creating a better opportunity to learn new samples from heterogeneous clients than the static NS. In addition, Fig. 9(b) shows the test accuracy of the FL models under the considered algorithms based on the CIFAR-10 dataset, where each client is assigned 3,000 heterogeneous training samples with five labels. We see that the proposed TP-DDPG algorithm converges to the highest accuracy of 0.93, while the accuracy is lower than 0.9 for all the benchmarks.

Fig. 10 reveals the effects of constraint (18g) that defines the maximum round for not selecting a user and the importance-oriented weighting scheme for edge model aggregation in (5). The proposed TP-DDPG is compared with three baselines;

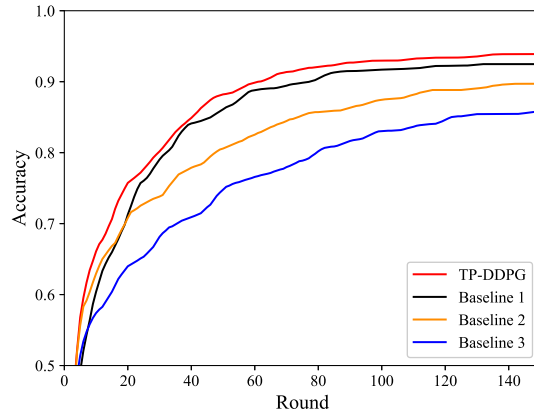


Fig. 10. Test accuracy versus cloud aggregation rounds.

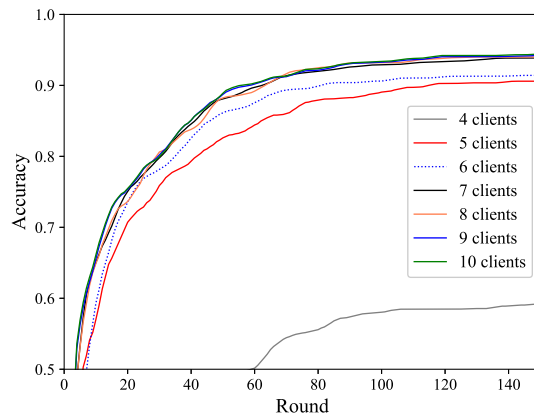


Fig. 11. Test accuracy under the TP-DDPG with different numbers of clients.

namely, i) Baseline 1, where constraint (18g) is removed from problem (18); ii) Baseline 2, where the edge model aggregation follows sample number-based weighting, as done in [21]; and iii) Baseline 3, where constraint (18g) is removed from problem (18) and the edge model aggregation follows the sample number-based weighting. Fig. 10 also shows that the baseline algorithms achieve worse accuracy than the TP-DDPG within the same number of cloud aggregation rounds. Without constraining the maximum number of rounds for not selecting a user, Baseline 1 may keep selecting clients with good channel conditions. A client with a critical dataset but poor channel conditions may not be chosen. This renders poor FL accuracy. By applying the importance-oriented weighting in the edge model aggregation, the proposed TP-DDPG effectively deals with the sample heterogeneity of clients and enhances the model accuracy, rather than concentrating only on the sample number of clients, as done in Baseline 2.

Fig. 11 plots the test accuracy of the FL model within 150 rounds of cloud aggregations under the proposed TP-DDPG, where the number of clients increases from 4 to 10. It is observed that with the same number of cloud aggregation rounds, the FL model can achieve finer accuracy with more clients

participating in learning. A significant accuracy improvement is observed when the number of clients is increased from 4 to 5. Nevertheless, the improvement decreases as the number of clients further increases.

VII. CONCLUSION

The learning delay and model accuracy of an FL task in an HFL system with energy harvesting clients were balanced using a joint resource allocation and client scheduling problem. We developed a new TP-DDPG algorithm that optimizes online energy management, computation and communication resource allocation, and client scheduling, adapting to varying wireless channels and renewable energy sources. The algorithm learns the selection of participating clients, and the CPU configurations and transmission powers of the clients. The rest of the decisions, i.e., client association and bandwidth allocation, and the reward of the DDPG are efficiently optimized by the new SCABA algorithm. Experimental results showed that the proposed TP-DDPG algorithm can achieve a higher test accuracy with a lower learning latency than the existing benchmarks.

REFERENCES

- [1] J. Hu, H. Zhang, B. Di, Z. Han, H. V. Poor, and L. Song, "Meta-material sensor based internet of things: Design, optimization, and implementation," *IEEE Trans. Commun.*, vol. 70, no. 8, pp. 5645–5662, 2022.
- [2] X. Chen, H. Wen, W. Ni, S. Zhang, X. Wang, S. Xu, and Q. Pei, "Distributed online optimization of edge computing with mixed power supply of renewable energy and smart grid," *IEEE Trans. Commun.*, vol. 70, no. 1, pp. 389–403, 2022.
- [3] H. B. McMahan, E. Moore, D. Ramage, S. Hampson, and B. A. Y. Arcas, "Communication-efficient learning of deep networks from decentralized data," 2016. [Online]. Available: <https://arxiv.org/abs/1602.05629>
- [4] S. Hu, X. Chen, W. Ni, E. Hossain, and X. Wang, "Distributed machine learning for wireless communication networks: Techniques, architectures, and applications," *IEEE Commun. Surveys Tuts.*, vol. 23, no. 3, pp. 1458–1493, 2021.
- [5] W. Y. B. Lim, N. C. Luong, D. T. Hoang, Y. Jiao, Y.-C. Liang, Q. Yang, D. Niyato, and C. Miao, "Federated learning in mobile edge networks: A comprehensive survey," *IEEE Commun. Surveys Tuts.*, vol. 22, no. 3, pp. 2031–2063, 2020.
- [6] M. Chen, Z. Yang, W. Saad, C. Yin, H. V. Poor, and S. Cui, "A joint learning and communications framework for federated learning over wireless networks," *IEEE Trans. Wireless Commun.*, vol. 20, no. 1, pp. 269–283, 2021.
- [7] T. Nishio and R. Yonetani, "Client selection for federated learning with heterogeneous resources in mobile edge," in *Proc. ICC*, 2019, pp. 1–7.
- [8] X. Mo and J. Xu, "Energy-efficient federated edge learning with joint communication and computation design," *J. Commun. Inf. Netw.*, vol. 6, no. 2, pp. 110–124, 2021.
- [9] Q. Zeng, Y. Du, K. Huang, and K. K. Leung, "Energy-efficient resource management for federated edge learning with CPU-GPU heterogeneous computing," *IEEE Trans. Wireless Commun.*, vol. 20, no. 12, pp. 7947–7962, 2021.
- [10] C. T. Dinh, N. H. Tran, M. N. H. Nguyen, C. S. Hong, W. Bao, A. Y. Zomaya, and V. Gramoli, "Federated learning over wireless networks: Convergence analysis and resource allocation," *IEEE/ACM Trans. Netw.*, vol. 29, no. 1, pp. 398–409, 2021.
- [11] J. Konečný, H. B. McMahan, F. X. Yu, P. Richtárik, A. T. Suresh, and D. Bacon, "Federated learning: Strategies for improving communication efficiency," *arXiv preprint arXiv:1610.05492*, 2016.
- [12] G. Zhu, Y. Wang, and K. Huang, "Broadband analog aggregation for low-latency federated edge learning," *IEEE Trans. Wireless Commun.*, vol. 19, no. 1, pp. 491–506, 2020.
- [13] S. Wang, Y. Hong, R. Wang, Q. Hao, Y.-C. Wu, and D. W. K. Ng, "Edge federated learning via unit-modulus over-the-air computation," *IEEE Trans. Commun.*, vol. 70, no. 5, pp. 3141–3156, 2022.
- [14] L. Yu, R. Albelaihi, X. Sun, N. Ansari, and M. Devetsikiotis, "Jointly optimizing client selection and resource management in wireless federated learning for internet of things," *IEEE Internet Things J.*, vol. 9, no. 6, pp. 4385–4395, Mar. 2022.
- [15] H. H. Yang, Z. Liu, T. Q. S. Quek, and H. V. Poor, "Scheduling policies for federated learning in wireless networks," *IEEE Trans. Commun.*, vol. 68, no. 1, pp. 317–333, 2020.
- [16] M. M. Wadu, S. Samarakoon, and M. Bennis, "Joint client scheduling and resource allocation under channel uncertainty in federated learning," *IEEE Trans. Commun.*, vol. 69, no. 9, pp. 5962–5974, 2021.
- [17] R. Hamdi, M. Chen, A. B. Said, M. Qaraqe, and H. V. Poor, "Federated learning over energy harvesting wireless networks," *IEEE Internet Things J.*, vol. 9, no. 1, pp. 92–103, Jan. 2022.
- [18] L. Liu, J. Zhang, S. Song, and K. B. Letaief, "Client-edge-cloud hierarchical federated learning," in *Proc. ICC*, 2020, pp. 1–6.
- [19] L. Liu, J. Zhang, S. H. Song, and K. B. Letaief, "Edge-assisted hierarchical federated learning with non-iid data," *ArXiv*, vol. abs/1905.06641, 2019.
- [20] X. Chen, Z. Li, W. Ni, X. Wang, S. Zhang, S. Xu, and Q. Pei, "Two-phase deep reinforcement learning of dynamic resource allocation and client selection for hierarchical federated learning," in *Proc. ICC*, 2022, pp. 518–523.
- [21] S. Luo, X. Chen, Q. Wu, Z. Zhou, and S. Yu, "HFEL: Joint edge association and resource allocation for cost-efficient hierarchical federated edge learning," *IEEE Trans. Wireless Commun.*, vol. 19, no. 10, pp. 6535–6548, 2020.
- [22] J. Feng, L. Liu, Q. Pei, and K. Li, "Min-max cost optimization for efficient hierarchical federated learning in wireless edge networks," *IEEE Trans. Parallel Distrib. Syst.*, vol. 33, no. 11, pp. 2687–2700, Nov. 2022.
- [23] B. Xu, W. Xia, J. Zhang, X. Sun, and H. Zhu, "Dynamic client association for energy-aware hierarchical federated learning," in *Proc. WCNC*. IEEE, 2021, pp. 1–6.
- [24] Z. Qu, R. Duan, L. Chen, J. Xu, Z. Lu, and Y. Liu, "Context-aware online client selection for hierarchical federated learning," 2021. [Online]. Available: <https://arxiv.org/abs/2112.00925>
- [25] Y. Deng, F. Lyu, J. Ren, Y. Zhang, Y. Zhou, Y. Zhang, and Y. Yang, "SHARE: Shaping data distribution at edge for communication-efficient hierarchical federated learning," in *Proc. IEEE 41st Int. Conf. Distrib. Comput. Syst.*, 2021, pp. 24–34.
- [26] W. Y. B. Lim, J. S. Ng, Z. Xiong, J. Jin, Y. Zhang, D. Niyato, C. Leung, and C. Miao, "Decentralized edge intelligence: A dynamic resource allocation framework for hierarchical federated learning," *IEEE Trans. Parallel Distrib. Syst.*, vol. 33, no. 3, pp. 536–550, 2021.
- [27] N. Mhaisen, A. Awad, A. Mohamed, A. Erbad, and M. Guizani, "Optimal user-edge assignment in hierarchical federated learning based on statistical properties and network topology constraints," *IEEE Trans. Netw. Sci. Eng.*, p. 1–1, 2021. [Online]. Available: <http://dx.doi.org/10.1109/TNSE.2021.3053588>
- [28] Z. Wang, H. Xu, J. Liu, H. Huang, C. Qiao, and Y. Zhao, "Resource-efficient federated learning with hierarchical aggregation in edge computing," in *Proc. IEEE Conf. Comput. Commun.*, 2021, pp. 1–10.
- [29] A. A. Abdellatif, N. Mhaisen, A. Mohamed, A. Erbad, M. Guizani, Z. Dawy, and W. Nasreddine, "Communication-efficient hierarchical federated learning for IoT heterogeneous systems with imbalanced data," *Future Generation Computer Systems*, vol. 128, pp. 406–419, 2022.
- [30] S. Liu, G. Yu, X. Chen, and M. Bennis, "Joint user association and resource allocation for wireless hierarchical federated learning with IID and non-IID data," *IEEE Trans. Wireless Commun.*, vol. 21, no. 10, pp. 7852–7866, Oct. 2022.
- [31] H. Sun, H. Tian, J. Zheng, and W. Ni, "Joint optimization of convergence and latency for hierarchical federated learning over wireless networks," *IEEE Wireless Commun. Lett.*, vol. 13, no. 3, pp. 691–695, Mar. 2024.
- [32] W. Wen, Z. Chen, H. H. Yang, W. Xia, and T. Q. Quek, "Joint scheduling and resource allocation for hierarchical federated edge learning," *IEEE Trans. Wireless Commun.*, vol. 21, no. 8, pp. 5857–5872, Aug. 2022.
- [33] T. Zhang, K.-Y. Lam, and J. Zhao, "Device scheduling and assignment in hierarchical federated learning for internet of things," *IEEE Internet Things J.*, vol. 11, no. 10, pp. 18449–18462, May 2024.
- [34] W. Y. B. Lim, J. S. Ng, Z. Xiong, D. Niyato, C. Miao, and D. I. Kim, "Dynamic edge association and resource allocation in self-organizing hierarchical federated learning networks," *IEEE J. Sel. Areas Commun.*, vol. 39, no. 12, pp. 3640–3653, Dec. 2021.
- [35] L. Su, R. Zhou, N. Wang, J. Chen, and Z. Li, "Low-latency hierarchical federated learning in wireless edge networks," *IEEE Internet Things J.*, vol. 11, no. 4, pp. 6943–6960, Feb. 2024.

- [36] T. Zhao, F. Li, and L. He, "DRL-based joint resource allocation and device orchestration for hierarchical federated learning in NOMA-enabled industrial IoT," *IEEE Trans. Ind. Inform.*, vol. 19, no. 6, pp. 7468–7479, Jun. 2023.
- [37] —, "DRL-based secure aggregation and resource orchestration in MEC-enabled hierarchical federated learning," *IEEE Internet Things J.*, vol. 10, no. 20, pp. 17 865–17 880, Oct. 2023.
- [38] Y. Xiao, X. Zhang, Y. Li, G. Shi, M. Krunz, D. N. Nguyen, and D. T. Hoang, "Time-sensitive learning for heterogeneous federated edge intelligence," *IEEE Trans. Mobile Comput.*, vol. 23, no. 2, pp. 1382–1400, Feb. 2024.
- [39] S. Abdulrahman, H. Tout, H. Ould-Slimane, A. Mourad, C. Talhi, and M. Guizani, "A survey on federated learning: The journey from centralized to distributed on-site learning and beyond," *IEEE Internet Things J.*, vol. 8, no. 7, pp. 5476–5497, 2021.
- [40] P. Villalobos, J. Sevilla, T. Besiroglu, L. Heim, A. Ho, and M. Hobbhahn, "Machine learning model sizes and the parameter gap," *arXiv preprint arXiv:2207.02852*, 2022.
- [41] F. Lai, X. Zhu, H. V. Madhyastha, and M. Chowdhury, "Oort: Efficient federated learning via guided participant selection," in *Proc. USENIX OSDI*, 2021, pp. 19–35.
- [42] G. Xia, J. Chen, C. Yu, and J. Ma, "Poisoning attacks in federated learning: A survey," *IEEE Access*, vol. 11, pp. 10 708–10 722, 2023.
- [43] Y. Zhang, D. Liu, M. Duan, L. Li, X. Chen, A. Ren, Y. Tan, and C. Wang, "FedMDS: An efficient model discrepancy-aware semi-asynchronous clustered federated learning framework," *IEEE Trans. Parallel Distrib. Syst.*, vol. 34, no. 3, pp. 1007–1019, 2023.
- [44] "Difference between NTP and PTP," 2021, <http://geeksforgEEKS.org/difference-between-ntp-and-ntp/>.
- [45] Z. Pan, H. Geng, L. Wei, and W. Zhao, "Adaptive client model update with reinforcement learning in synchronous federated learning," in *Prof. ITNAC*, 2022, pp. 155–157.
- [46] B. Xu, W. Xia, W. Wen, P. Liu, H. Zhao, and H. Zhu, "Adaptive hierarchical federated learning over wireless networks," *IEEE Trans. Veh. Technol.*, vol. 71, pp. 2070–2083, 2022.
- [47] C. Qiu, Y. Hu, Y. Chen, and B. Zeng, "Deep deterministic policy gradient (DDPG)-based energy harvesting wireless communications," *IEEE Internet Things J.*, vol. 6, no. 5, pp. 8577–8588, 2019.
- [48] R. Ghaemi, "Robust model based control of constrained systems." Ph.D. dissertation, Dept. Elect. Eng., Univ. Michigan, Ann Arbor, MI, USA, 2010.
- [49] S. Hu, X. Yuan, W. Ni, X. Wang, and J. Abbas, "Visual-based moving target tracking with solar-powered fixed-wing UAV: A new learning-based approach," *IEEE Trans. Intell. Transp. Syst.*, accepted, 2024.
- [50] B. Yin, Z. Chen, and M. Tao, "Joint user scheduling and resource allocation for federated learning over wireless networks," in *Proc. GLOBECOM*, 2020, pp. 1–6.